Journal of Biomolecular NMR (2006) 35: 261–274
DOI 10.1007/s10858-006-9041-x

Article

Alternate-site isotopic labeling of ribonucleotides for NMR studies of ribose conformational dynamics in RNA

James E. Johnson Jr, Kristine R. Julien & Charles G. Hoogstraten*
Department of Biochemistry & Molecular Biology, Michigan State University, 212 Biochemistry Building, East Lansing, MI 48824, USA

Received 17 March 2006; Accepted 2 June 2006

Key words: alternate-site, dynamics, glucose-6-phosphate dehydrogenase, isotope labeling, ribose, RNA

Abstract

Heteronuclear NMR spin relaxation studies of conformational dynamics are coming into increasing use to help understand the functions of ribozymes and other RNAs. Due to strong ^{13}C–^{13}C magnetic interactions within the ribose ring, however, these studies have thus far largely been limited to ^{13}C and ^{15}N resonances on the nucleotide base side chains. We report here the application of the alternate-site ^{13}C isotopic labeling scheme, pioneered by LeMaster for relaxation studies of amino acid side chains, to nucleic acid systems. We have used different strains of *E. coli* to prepare mononucleotides containing ^{13}C label in one of two patterns: Either C1′ or C2′ in addition to C4′, termed (1′/2′,4′) labeling, or nearly complete labeling at the C2′ and C4′ sites only, termed (2′,4′) labeling. These patterns provide isolated ^{13}C–^{1}H spin systems on the labeled carbon atoms and thus allow spin relaxation studies without interference from ^{13}C–^{13}C scalar or dipolar coupling. Using relaxation studies of AMP dissolved in glycerol at varying temperature to produce systems with correlation times characteristic of different size RNAs, we demonstrate the removal of errors due to ^{13}C–^{13}C interaction in T_1 measurements of larger nucleic acids and in $T_{1\rho}$ measurements in RNA molecules. By extending the applicability of spin relaxation measurements to backbone ribose groups, this technology should greatly improve the flexibility and completeness of NMR analyses of conformational dynamics in RNA.

Abbreviations: AMP – adenosine 5′-monophosphate; CMP – cytidine 5′-monophosphate; CPMG – Carr-Purcell-Meiboom-Gill; CSA – chemical shift anisotropy; G3P – glyceraldehyde-3-phosphate; G6P – glucose-6-phosphate; G6PDH – glucose-6-phosphate dehydrogenase; HSQC – heteronuclear single-quantum correlation; R5P – ribose-5-phosphate; rNMP – ribonucleoside 5′-monophosphate; TCA – tricarboxylic acid

Introduction

Heteronuclear NMR spin relaxation has become a major tool for the study of conformational dynamics in biological macromolecules, both on the picosecond–nanosecond (Wagner and Wüthrich, 1986; Dayie et al., 1996; Palmer, 2004) and microsecond–millisecond (Szyperski et al., 1993; Palmer et al., 2001; Akke, 2002) timescales. Following the initial development of the technology in proteins (Kay et al., 1989), applications to ^{15}N and ^{13}C resonances of RNA and DNA have expanded as the uniform isotopic labeling of these nucleic acids has become routine (King et al., 1995; Akke et al., 1997; Hall and Tang, 1998; Hoogstraten et al., 2000; Dayie et al.,

*To whom correspondence should be addressed. E-mail: hoogstr3@msu.edu

2002; Boisbouvier et al., 2003; Blad et al., 2005; Duchardt and Schwalbe, 2005; Shajani and Varani, 2005). In nucleic acids, however, interference from strong ^{13}C–^{13}C magnetic interactions within the backbone ribose ring has largely limited such studies to protonated ^{15}N and ^{13}C atoms on the nucleotide base side chain, with some limited data available on relatively isolated C1′ sites (see inset to Figure 1 for numbering). Approaches to the problem of ^{13}C–^{13}C interference in nucleic acids have included the acquisition of data at natural isotopic abundance (Borer et al., 1994; Spielmann, 1998; Isaacs and Spielmann, 2001; Isaacs et al., 2002) or random fractional ^{13}C labeling (Hines et al., 1993; Hines et al., 1994; Kojima et al., 1998; Boisbouvier et al., 1999; Kojima et al., 2001; Kishore et al., 2005), requiring a significant sacrifice in experimental sensitivity; the measurement of cross-correlated relaxation rates (Boisbouvier et al., 1999; Dayie et al., 2002); and the labor-intensive synthesis of selectively labeled nucleotide precursors (Williamson and Boxer, 1989; Gaudin et al., 1995; SantaLucia et al., 1995; Gaudin et al., 1997; Hatala et al., 2001). In favorable cases, complementary data may be obtained using spin-relaxation studies on backbone ^{31}P resonances (Catoire, 2004). Given the importance of conformational dynamics to the function of ribozymes (Pley et al., 1994; Hoogstraten et al., 1998; Ke et al., 2004) and other RNA systems (Treiber and Williamson, 2001; Perez-Canadillas and Varani, 2001; al-Hashimi, 2005), a general and facile method to extend ^{13}C spin relaxation studies of RNA to the backbone ribose carbon resonances is an important research goal.

In the work reported here, we have addressed this issue by adapting the alternate-site labeling protocol introduced by the LeMaster group for studies of amino-acid side chain carbon sites (LeMaster and Cronan, 1982; LeMaster and Kushlan, 1996). In this scheme, appropriate combinations of particular metabolic ablations in *E. coli* and specifically labeled feedstocks are used to biosynthetically produce metabolites with ^{13}C atoms directly bonded only to ^{12}C atoms. Alternate-site protein labeling has recently found use in solid-state NMR studies of protein structure by allowing the measurement of small dipolar couplings in the absence of otherwise dominant one-bond interactions (Castellani et al., 2002, 2003). In solution, such labeling patterns remove contributions to relaxation due to one-bond carbon–carbon scalar and dipolar couplings and allow the analysis of a given ^{13}C resonance, with its directly attached ^{1}H, as an isolated two-spin system. For nucleotides, the preparation of alternate-site labeled samples follows well-established procedures, differing from standard methods to prepare uniformly labeled nucleotides (Batey et al., 1992; Nikonowicz et al., 1992) only in the choice of bacterial strain and carbon source. Indeed, the procedure is in some sense more general than the alternate-site labeling of proteins, since the transformation of a bacterial strain that may not be ideal for the expression of the protein of interest is not necessary.

The genotype of *E. coli* strain DL323 (Coli Genetic Stock Center #7538) (LeMaster and Kushlan, 1996) includes mutations in the succinate dehydrogenase (*sdh*) and malate dehydrogenase (*mdh*) genes, resulting in an interruption of the tricarboxylic acid (TCA) cycle. In metabolites derived from TCA cycle intermediates, this disruption prevents the isotope scrambling that otherwise arises from the symmetry of succinic acid. When grown on 2-^{13}C-glycerol as the sole carbon source, DL323 results in favorable ^{12}C–^{13}C–^{12}C isotope labeling patterns in a number of aliphatic and aromatic amino acid side chains (LeMaster and Kushlan, 1996). In nucleic acids, alterations to the labeling patterns of pyrimidine side chains are expected due to the specific labeling of precursor aspartic acid. No direct effects, however, are expected on observed labeling patterns within the ribose group.

Nucleotides are synthesized from ribose-5-phosphate derived via the two branches of the pentose phosphate pathway (Figure 1) (Nelson and Cox, 2004). In the oxidative pentose phosphate pathway, glucose-6-phosphate (G6P) is irreversibly converted to ribose-5-phosphate (R5P) by a series of four enzymes beginning with glucose-6-phosphate dehydrogenase (G6PDH). In the process, C-1 of G6P is lost as CO_2. In the nonoxidative branch of the pentose phosphate pathway, by contrast, the combined action of transketolase and transaldolase reversibly converts the equivalent of five molecules of three-carbon compounds into three molecules of five-carbon R5P and xylulose-5-phosphate, which are mutually interconvertible via ribulose-5-phosphate. [We note that the latter reactions are the reverse of the canonical description of the nonoxidative pathway (Nelson and Cox,

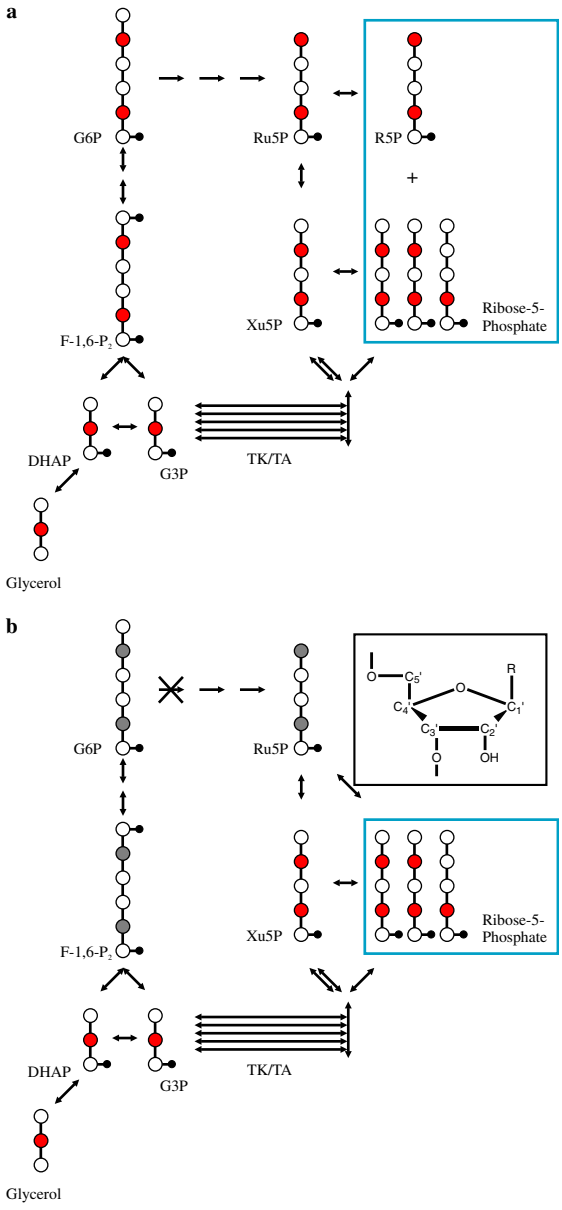

Figure 1. Pathways for synthesis of ribose-5-phosphate in wildtype and mutant *E. coli*. Circles represent carbon atoms in the indicated carbohydrate intermediates; colored shading indicates ^{13}C label. Small black circles show the location of phosphate groups. G6P, glucose-6-phosphate; F-1,6-P_2, fructose-1,6-bisphosphate; DHAP, dihydroxy acetone phosphate; G3P, glyceraldehyde-3-phosphate; Ru5P, ribulose-5-phosphate; Xu5P, xylulose-5-phosphate; R5P, ribose-5-phosphate; TK/TA, transketolase and transaldolase reactions. (a) production of multiple isotopomers of R5P in wildtype or DL323 cells (1′/2′,4′ labeling); (b) specific production of labeled R5P in *zwf* bacterial strains (2′,4′ labeling). The deleted enzyme (glucose-6-phosphate dehydrogenase) is indicated and the eliminated pathway for R5P production is converted to grayscale. The inset shows the numbering scheme used for RNA ribose carbons.

2004), used to recycle R5P into glycolytic intermediates. Under certain conditions, however, metabolic flux in this retrograde direction is significant, as demonstrated below.] These two pathways of ribose formation result in different patterns of labeling in R5P when a given specifically labeled precursor (e.g., 2-^{13}C-glycerol or 1,3-$^{13}C_2$-glycerol) is used as a sole carbon source (Figure 1a). In wildtype or DL323 *E. coli*, therefore, the distribution of label in nucleotides will depend on the partitioning of carbon flux between the two branches of the pentose phosphate pathway. We reasoned that bacteria deficient in the oxidative pentose phosphate pathway, such as *zwf* strains with mutations in the glucose-6-phosphate dehydrogenase gene (Fraenkel, 1968), would give well-defined labeling patterns since only the transketolase/transaldolase route is available for the production of R5P (Figure 1b). A metabolic network analysis of *zwf* mutants in *E. coli* predicted essentially wildtype cell growth and derivation of R5P strictly via transketolase and transaldolase (Edwards and Palsson, 2000). Indeed, such strains are shown below to give useful alternate-site labeling patterns in nucleotide ribose groups when grown on an appropriate carbon source.

In this work, we use *E. coli* strains deficient in either the TCA cycle (DL323) or the oxidative pentose phosphate pathway (*zwf* strains K10-1516 and DF2001) to achieve the biosynthesis of ribonucleotides with a variety of favorable alternate-site isotopic labeling patterns. This work thus builds on the report of Hoffman and Holland (1995) who used single-site labeled acetate and wildtype *E. coli* to achieve a partial alternate-site pattern in nucleotides. We further use a comparison of T_1 and $T_{1\rho}$ relaxation at a variety of rotational correlation times in alternate-site labeled vs. uniformly labeled nucleotides to demonstrate that errors due to ^{13}C–^{13}C interactions are in fact significant in uniformly labeled samples. The ability to acquire reliable relaxation data on ribose carbon resonances using easily-prepared samples promises to open a new window into the dynamic characteristics of RNA.

Materials and methods

Reagents and bacterial strains

Chemicals were purchased from Sigma-Aldrich at the highest purity available unless otherwise noted. Specifically labeled glycerol (99% ^{13}C) and glucose (99% ^{13}C) and d_8-glycerol (98% ^{2}H) were obtained from Cambridge Isotope Laboratories. Uniformly $^{15}N/^{13}C$-labeled adenosine 5′-monophosphate (AMP) was purchased from Spectra Stable Isotopes. The following *E. coli* strains were obtained from the Coli Genetic Stock Center at Yale: DL323 (CGSC #7538; F^- *sdh-1 mdh-2 rph-1*), K10-1516 (#4858; Hfr *fhu22 zwf-2 relA1 pfk-10*), and DF2001 (#4874; Hfr *garB10 fhuA22 ompF627 zwf-2 fadL701 relA1 pit-10 spoT1 rrnB-2 mcrB9999 creC510*). Strains were resuscitated in LB medium and stored at −80 °C in equimolar amounts of 60% glycerol.

Nucleotide biosynthesis

Specifically labeled nucleotide 5′-monophosphates (rNMPs) were obtained via total RNA preparations from appropriate *E. coli* cultures grown on minimal (M9) media with 1 g/l of a defined, specifically labeled carbon source using standard methods (Batey et al., 1995). In our hands, the *sdh*/*mdh* strain DL323 is substantially handicapped in growth rate on glycerol compared to wildtype, but reaches a reasonable cell density at stationary phase. In contrast, the *zwf* strains K10-1516 and DF2001 are essentially indistinguishable from wildtype in growth characteristics. In a typical prep, 1 l of culture yielded approximately 4 g of wet cells and 700 A_{260} units of rNMPs. Individual nucleotides were separated using a polyethyleneimine anion exchange column (Poros) with a starting buffer of 25 mM ammonium formate, pH 3.0, and eluted with a linear gradient of 500 mM ammonium formate, pH 2.5 (Batey et al., 1995). NMR samples of nucleotides and nucleotide mixtures were prepared to a final concentration of 2 mM in 10 mM sodium phosphate buffer, pH 7.5, and exchanged into D_2O using repeated lyophilization. For relaxation rate measurements, 2 mM samples of specifically labeled and commercial uniformly labeled AMP were resuspended in d_8-glycerol and a capillary NMR tube insert (Wilmad) filled with 99.96% D_2O was used for spectrometer lock.

NMR spectroscopy and data analysis

All spectra were obtained on a 600 MHz Varian UnityInova spectrometer. Nucleotide mixtures were characterized using heteronuclear single quantum correlation (HSQC) spectra optimized for resolution in the t_1 (^{13}C) dimension. Relaxation rates (R_1 and $R_{1\rho}$) were determined using slightly modified, non-constant-time versions of published sequences (Yamazaki et al., 1994) as described previously (Hoogstraten et al., 2000). Spectra were obtained in one-dimensional (^{1}H) mode for monomer samples by omitting the incremented (t_1) delay. For $R_{1\rho}$, data for C2′ and C4′ were collected separately with the ^{13}C carrier placed on exact resonance in each case. Error bars on intensity measurements were determined by repeating a single time point three times. Rate constants were determined by nonlinear fitting of the intensity data to a single exponential using Igor Pro 4.0 (WaveMetrics). Errors in rates are those derived from the covariation matrix as reported by the nonlinear fitting routine. Apparent rotational correlation times τ_m at a given temperature were calculated from the $R_{1\rho}/R_1$ ratio for the C2′ resonance in (2′,4′)-^{13}C AMP taking into account ^{1}H–^{13}C dipole–dipole and ^{13}C chemical shift anisotropy mechanisms (Kay et al., 1989) using a C–H bond length of 1.10 Å (Klooster et al., 1991) and a chemical shift anisotropy value ($\sigma_{\parallel} - \sigma_{\perp}$) of 40 ppm.

Results

Alternate-site labeling of nucleoside monophosphates

In order to implement the alternate-site labeling scheme in ribonucleotides, we grew *E. coli* strain DL323, deficient in the TCA cycle enzymes succinate dehydrogenase and malate dehydrogenase, on 1,3-$^{13}C_2$-glycerol and separately on 2-^{13}C-glycerol, and the *zwf* (glucose-6-phosphate dehydrogenase mutant) strains K10-1516 and DF2001 on 2-^{13}C-glycerol. The two *zwf* strains gave equivalent isotopic labeling patterns; only results from strain K10-1516 are illustrated here.

Glycerol used as a carbon source enters central metabolism via the glycerol kinase and glycerol

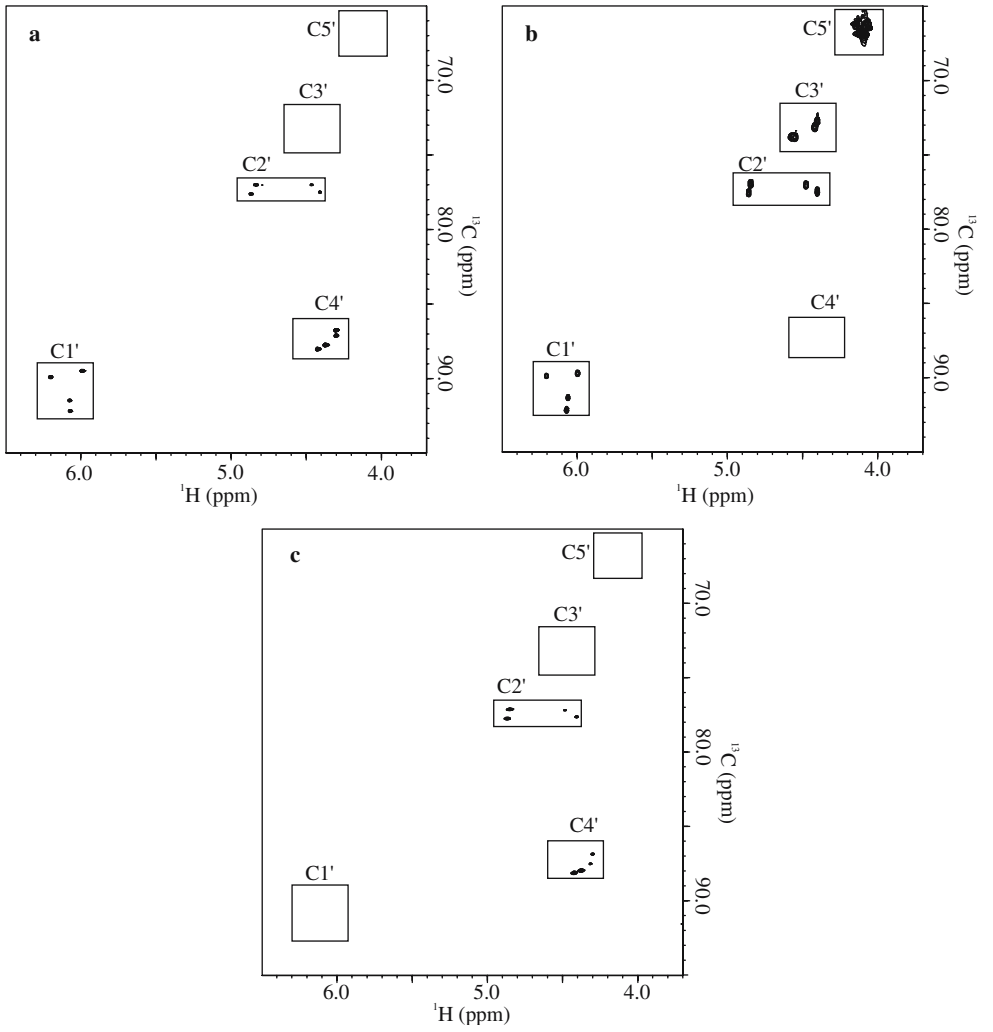

Figure 2. Production of specifically labeled rNMPs. ^{1}H–^{13}C HSQC spectra (ribose region) of mixtures of the four rNMPs isolated from bacterial culture. (a) DL323 *E. coli* grown on 2-^{13}C-glycerol; (b) DL323 *E. coli* grown on 1,3-$^{13}C_2$-glycerol; (c) K10-1516 (*zwf*) *E. coli* grown on 2-^{13}C-glycerol.

phosphate dehydrogenase reactions as dihydroxyacetone phosphate, which can be converted to glyceraldehyde-3-phosphate (G3P) by triosephosphate isomerase. As discussed above, the labeling pattern observed in R5P will depend on the pathway by which G3P is converted to the five-carbon level (Figure 1). If G3P is converted to G6P via gluconeogenesis and then to R5P via G6PDH and the oxidative pentose phosphate pathway, C-1 and C-4 of R5P will be derived from the central C-2 carbon of glycerol. By contrast, if one equivalent of G3P and two equivalents of gluconeogenesis-derived fructose-6-phosphate are converted to five-carbon sugars by transketolase and transaldolase, the result will be two equivalents of R5P in which C-2 and C-4 are derived from C-2 of glycerol and one equivalent of R5P in which only C-4 is derived from C-2 of glycerol. In wildtype or DL323 *E. coli*, both of these pathways should be active, and the partitioning of carbon flux was not known *a priori*. For *zwf* strains, only R5P produced via transketolase and transaldolase was expected.

In Figure 2, we show ^{1}H–^{13}C HSQC NMR spectra for mixtures of the four rNMPs derived from *E. coli* grown as described above. For DL323, growth on 2-^{13}C-glycerol results in strong labeling at C4′ and a near absence of label at C3′ and C5′, whereas growth on 1,3-$^{13}C_2$-glycerol

results in strong labeling at C3′ and C5′ and a near absence of label at C4′, as expected. Both samples, however, show partial labeling at both C1′ and C2′, indicating that substantial amounts of R5P have been produced via both the G6PDH and transketolase/transaldolase pathways. In the *zwf* strain K10-1516 grown on 2-^{13}C-glycerol, by contrast, ^{13}C label is essentially absent at all sites except for C2′ and C4′, consistent with dominant production of R5P via transketolase and transaldolase operating as shown in Figure 1b. The latter pattern is consistent with the successful production of isolated two-spin systems for ribose C2′ and C4′ resonances.

The results may be further analyzed by considering the exact isotopomers observed. To this end, we isolated AMP from DL323 and K10-1516 grown on 2-^{13}C-glycerol and examined its ^{1}H–^{13}C and ^{13}C–^{13}C NMR multiplet patterns. In Figure 3, we show the ribose region of one-dimensional (1D) NMR spectra of these two samples, taken without ^{13}C decoupling, in comparison to uniformly labeled AMP acquired both with and without ^{13}C decoupling. These spectra confirm the essentially complete ^{13}C labeling of C4′ and absence of label at C3′ and C5′ for both 2-^{13}C-glycerol preps. For the DL323 prep, both C1′ and C2′ are partially labelled, whereas, for the *zwf* strain, C1′ is nearly completely unlabeled and C2′ is $> 75\%$ labeled.

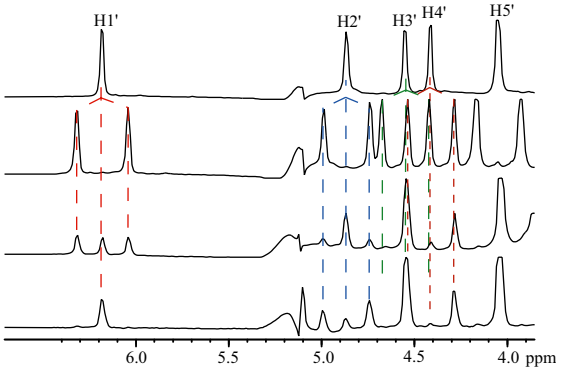

Figure 3. Fraction of ^{13}C label at individual sites. One-dimensional ^{1}H NMR spectra of AMP acquired at 5 °C. The top spectrum is a ^{13}C-decoupled spectrum of uniformly labeled material shown for reference; the remaining spectra were acquired without ^{13}C decoupling. Top to bottom, uniformly labeled AMP (decoupled); uniformly labeled AMP (not decoupled); AMP isolated from *E. coli* DL323 grown on 2-^{13}C-glycerol (1′/2′,4′ labeling); AMP isolated from *E. coli* K10-1516 grown on 2-^{13}C-glycerol (2′,4′ labeling).

We completed the isotopomer analysis by reference to ^{13}C–^{13}C coupling patterns observed in the indirect dimension of HSQC spectra of isolated AMP (Figure 4). The triplet structure at both the C2′ and C4′ resonances due to two equivalent ^{13}C–^{13}C couplings in the uniformly labeled sample is clearly visible. For the alternate-site labeled nucleotides, however, C4′ is completely singlet in both cases, consistent with the lack of label at C3′ and C5′. C2′ is also fully isolated from other ^{13}C nuclei in the K10-1516 prep, whereas the DL323 growth showed a small amount of residual doublet contribution, arising from isotopomers with ^{13}C2′ and either ^{13}C1′ or ^{13}C3′, but not both. By combining all the data, we extracted the isotopomer fractional populations given in Table 1.

We also determined the pyrimidine ring isotopomers present in the various preps via multiplet analysis of 5′-cytidine monophosphate (CMP) (data not shown). DL323, due to the interruption of the TCA cycle and consequent specific labeling pattern on aspartic acid, yielded ca. 90% ^{13}C5–^{12}C6-CMP when grown on 1,3-$^{13}C_2$-glycerol, and ca. 90% ^{12}C5–^{13}C6-CMP when grown on 2-^{13}C-glycerol. K10-1516, by contrast, yielded roughly 50% ^{13}C at each site when grown on either glycerol species. We note, however, that the ^{13}C multiplet pattern was essentially pure singlet in each case.

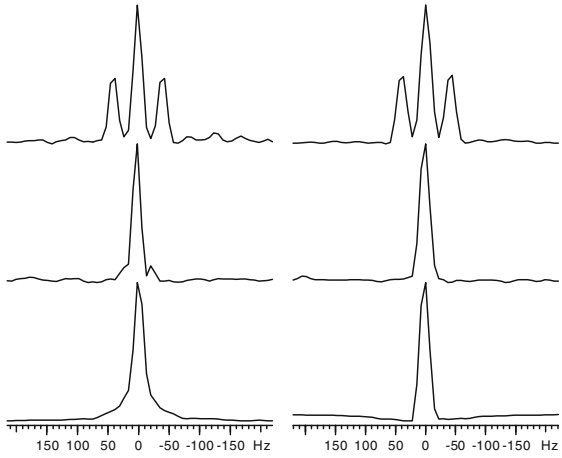

Figure 4. ^{13}C–^{13}C multiplet patterns in HSQC spectra. Sections parallel to the ^{13}C frequency axis through the (a) C2′ and (b) C4′ resonance of AMP. Top, commercial uniformly labeled material; middle, (1′/2′,4′) labeling from DL323 bacteria, showing a small amount of residual doublet in the C2′ case; bottom, (2′,4′) labeling from K10-1516 (*zwf*) bacteria, showing essentially complete isolation of the corresponding ^{13}C resonances.

Table 1. Isotopomeric species obtained in nucleotide preparations

E. coli strain	Carbon source	Isotopomer	Yield (%)
DL323 (*sdh, mdh*)	1,3-$^{13}C_2$-glycerol	1′,3′,5′-$^{13}C_3$-ribose	25
		2′,3′,5′-$^{13}C_3$-ribose	55
		1′,2′,3′,5′-$^{13}C_4$-ribose	10
		3′,5′-$^{13}C_2$-ribose	5
		Various $^{13}C_1$-ribose	< 5
DL323 (*sdh, mdh*)	2-^{13}C-glycerol	1′,4′-$^{13}C_2$-ribose	55
		2′,4′-$^{13}C_2$-ribose	30
		1′,2′,4′-$^{13}C_3$-ribose	< 5
		4′-^{13}C-ribose	10
		Various $^{13}C_1$-ribose	< 5
K10-1516	2-^{13}C-glycerol	2′,4′-$^{13}C_2$-ribose	80
		4′-^{13}C-ribose	5
		1′,4′-$^{13}C_2$-ribose	5
		1′,2′,4′-$^{13}C_2$-ribose	5
		Various $^{13}C_1$-ribose	< 5

Specific labeling at the C3′ site

As discussed more fully below, the above procedures provide spectroscopically useful isolation of the C4′, C2′, and possibly C1′ sites. The C3′ site, however, has been predicted to undergo the greatest chemical shift change upon C3′-endo/C2′-endo pseudorotation (Ebrahimi et al., 2001; Rossi and Harbison, 2001), and thus may be the most sensitive spin relaxation probe of conformational exchange processes. We were therefore interested in a procedure giving rise to a fully isolated ^{13}C spin at this site. We obtained this pattern by growing wildtype *E. coli* on 4-^{13}C-glucose. Assuming that wildtype *E. coli* grown on glucose obtains all its ribose via R5P derived from the oxidative branch of the pentose phosphate pathway, this scheme should result in pure 3′-^{13}C-rNMPs. This prediction is verified by the one-dimensional NMR spectrum of AMP derived from a small-scale preparation of this type shown in Figure 5. This procedure thus provides a readily available route to nucleotides with the ribose groups isotope labeled at C3′ only.

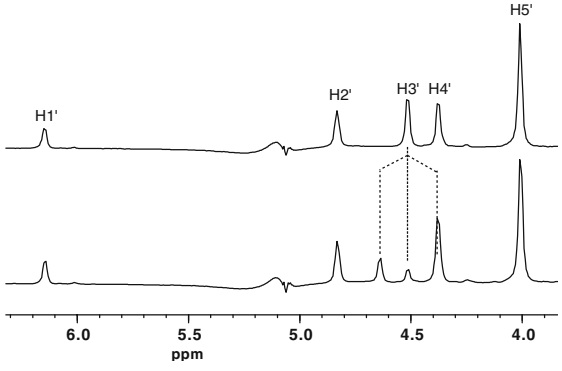

Figure 5. Isolation of the C3′ resonance. ^{13}C-decoupled (top) and undecoupled (bottom) NMR spectra of AMP prepared from wildtype *E. coli* grown on 4-^{13}C-glucose.

Relaxation analysis of nucleotides

With alternate-site labeled NMPs in hand, we proceeded to compare the spin relaxation behavior of specifically and uniformly labeled nucleotides. This analysis not only demonstrates the properties of the alternate-site labeled nucleotides but confirms the magnitude of the errors obtained when uniformly labeled materials are used. For example, any difference in the T_1 or $T_{1\rho}$ of C2′ or C4′ in $^{13}C_5$-rAMP compared to 2′,4′-$^{13}C_2$-rAMP could arise only from the presence of ^{13}C1′, ^{13}C3′, or ^{13}C5′. Since these ^{13}C–^{13}C interactions are not accounted for in the usual procedures of data analysis and interpretation, any such differences will lead to errors in the derived parameters describing the dynamic properties of the molecule. Thus, we interpret any difference in relaxation between specifically and uniformly labeled samples as evidence for inaccuracies in the analysis of conventional uniformly labeled material.

Table 2. ^{13}C relaxation rates for AMP dissolved in glycerol-d_8

T (°C)	(2′,4′)-$^{13}C_2$		Uniform ^{13}C	
	C2′	C4′	C2′	C4′
^{13}C R_1 (s^{-1})				
30	1.48 ± 0.05	1.13 ± 0.02	1.59 ± 0.07	1.29 ± 0.05
25	1.1 ± 0.1	0.90 ± 0.08	1.12 ± 0.01	1.07 ± 0.04
20	0.95 ± 0.06	0.67 ± 0.02	0.79 ± 0.02	0.84 ± 0.04
15	0.9 ± 0.2	1.9 ± 0.1	0.4 ± 0.2	0.9 ± 0.1
^{13}C $R_{1\rho}$ (s^{-1}), on-resonance[a]				
$\gamma B_1/2\pi = 2980$ Hz				
30	25 ± 1	37.0 ± 0.9	25.8 ± 0.7	47 ± 3
25	38 ± 4	53 ± 3	29 ± 4	57 ± 2
20	70 ± 10	140 ± 20	67 ± 3	120 ± 20
15	150 ± 40	nd[b]	90 ± 10	nd[b]
$\gamma B_1/2\pi = 1550$ Hz				
30	22 ± 2	36 ± 2	23 ± 1	38 ± 2

[a]Data for C2′ and C4′ resonances were collected separately with the ^{13}C transmitter placed on exact resonance in each case. [b]Data could not be analyzed due to interference from ^{13}C satellites of the strong residual glycerol signal.

To perform this comparison at a range of rotational correlation times, corresponding to various sizes of RNA molecules, we adopted a procedure used by the Kay group to analyze the effect of various labeling patterns in amino acids (Yamazaki et al., 1994). Specifically, we prepared NMR samples of rAMP dissolved in deuterated glycerol, using a capillary filled with D_2O to achieve spectrometer lock. The strongly temperature-dependent viscosity of glycerol results in mononucleotides that tumble with a wide range of rotational correlation times as the temperature is varied. We could therefore simulate the effects of uniform *vs*. specific labeling on RNA molecules of a wide variety of molecular weights with a single pair of easily prepared samples.

The extracted relaxation rates are collected in Table 2. Using the ratio of T_1 to $T_{1\rho}$ for C2′ of the alternate-site nucleotide, we estimate that the four temperatures of 30, 25, 20, and 15 °C correspond to rotational correlation times of 5.4, 7.8, 11.8, and 16.9 ns, respectively, for AMP. Assuming a linear scaling of correlation time with molecular weight and taking 6.0–6.4 ns as the correlation time for a 30-nucleotide RNA stem loop in D_2O at 25 °C (Hoogstraten et al., 2000; Blad et al., 2005), the C2′ resonance in our sample shows relaxation behavior roughly characteristic of RNAs of 26, 38, 57, and 82 nucleotides, respectively, at the four temperatures used. In cases for which both measurements are available, C4′ resonances generally show faster longitudinal and slower transverse relaxation than C2′, corresponding to a smaller apparent rotational correlation time. This discrepancy may arise from differences in average bond length or chemical shift tensor for these two atoms [indeed, Bax and coworkers have recently reported widely variant chemical shift tensor spans for different ribose carbons in RNA (Bryce et al., 2005)] or to differences in the respective spectral densities. It will be of interest to compare the behavior of C2′ and C4′ resonances in structured RNA molecules, possibly including cross-correlated relaxation analyses to distinguish static from dynamic effects (Boisbouvier et al., 1999).

Table 2 and Figure 6 compare the effect of varying temperature, and thus correlation time, on longitudinal relaxation rates in specifically (2′,4′-$^{13}C_2$) labeled AMP, derived from *E. coli* strain K10-1516 grown on 2-^{13}C-glycerol, with commercial uniformly labeled nucleotide. The R_1 relaxation rates for the two samples are essentially identical at a correlation time of 5.4 ns, diverging as the correlation time increases until they ultimately differ by more than a factor of two at 16.9 ns (Figure 6, Table 2). That is, measurements in the uniformly labeled sample give accurate results for R_1 under conditions corresponding to short RNA hairpins, but give rise to increasingly

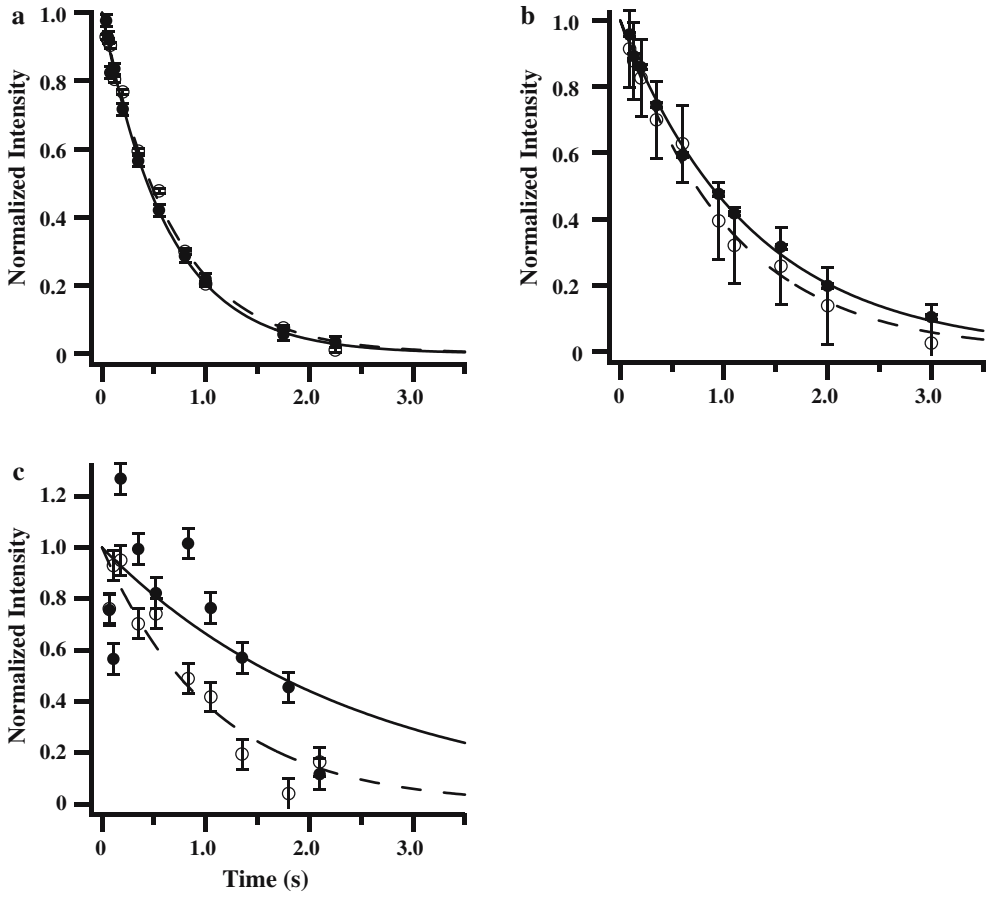

Figure 6. Longitudinal relaxation of AMP in glycerol. T_1 decay curves for C2′ of (solid line) uniformly labeled and (dashed line) 2′,4′-^{13}C labeled AMP at (a), 30 °C; (b), 20 °C; (c), 15 °C. Extracted rate constants are given in Table 2.

significant inaccuracies as the apparent molecular size increases. This observation is in agreement with the results of Bax and coworkers, who showed that the contributions both of ^{13}C–^{13}C terms in the autorelaxation rate of ribose carbons and of ^{13}C–^{13}C cross relaxation are negligible for correlation times of less than 4 ns (Boisbouvier et al., 2003). Both of these effects will increase in significance relative to ^{1}H–^{13}C contributions to ^{13}C autorelaxation as the correlation time increases (see below).

For $T_{1\rho}$, the situation is somewhat different, as the most serious potential errors due to ^{13}C–^{13}C interactions arise from magnetization transfer via the Hartmann–Hahn mechanism during the spin-lock period (Boisbouvier et al., 2003). The rates of Hartmann–Hahn transfer will be a complex function of the topology of the spin system, the ^{13}C chemical shifts for a particular nucleotide, and the magnitude and frequency of the spin-lock field used (Bax and Davis, 1985). For AMP dissolved in glycerol, we indeed observe agreement between measurements in uniform and alternate-site labeled nucleotides under some combinations of resonance studied, spin-lock power, and correlation time (Figure 7a). In other cases, however, we observe discrepancies of up to 50%, representing significant inaccuracies in the uniform-labeling data. Indeed, for the case of the C4′ resonance at 30 °C, we observe agreement among measurements at two different spin-lock powers in the alternate-site sample and at the lower spin-lock power in the uniformly labeled sample. At the higher spin-lock power, however, we observe an increased rate of transverse relaxation in the uniformly labeled sample, implying that Hartmann–Hahn transfers

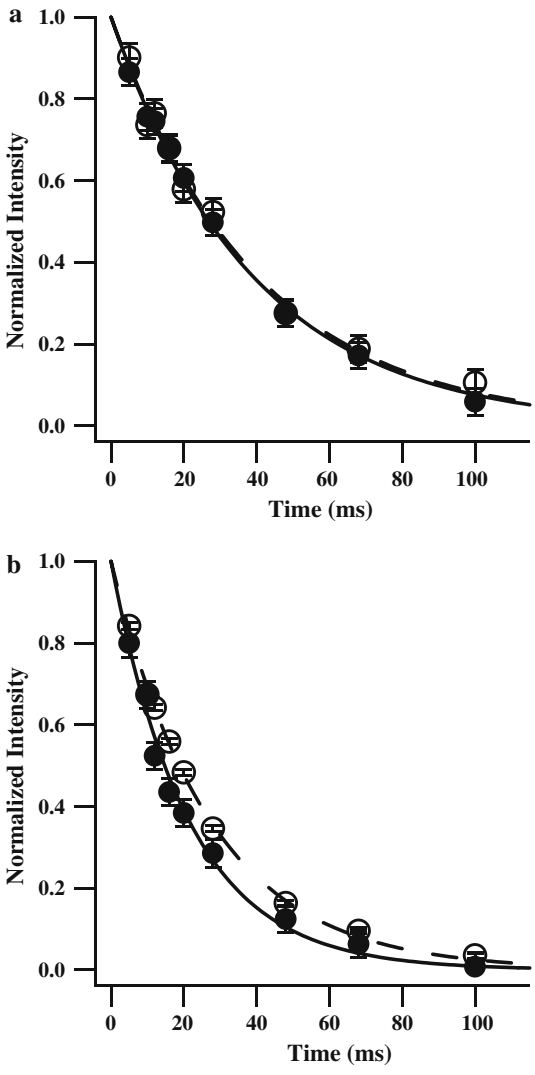

Figure 7. Transverse relaxation of AMP in glycerol. On-resonance $T_{1\rho}$ decay curves for (solid line) uniformly labeled and (dashed line) 2′,4′-^{13}C labeled AMP at 30 °C and 2980 Hz spin-lock power. (a) C2′ resonance; (b) C4′ resonance. Extracted rate constants are given in Table 2.

have adversely affected the latter measurement (Figure 7b). In preliminary experiments using ^{13}C spin-lock fields applied away from exact resonance, which will be the situation in practical cases for structured RNA molecules, we observe some examples of increased differences between specifically and uniformly labeled samples (data not shown). It is worth noting that the quantitative interpretation of the results in Figure 7 is not obvious; the simple expressions derived by Bax and Davis (1985) for the maximal amount of Hartmann–Hahn transfer under continuous-wave irradiation do not predict measurable interaction of C4′ with either C3′, at a relative offset of 14.2 ppm, or C1′, at a relative offset of 2.0 ppm and a coupling constant of 0.8 Hz (measured in the ribonucleoside) (Kline and Serianni, 1990). Since the pattern of relative changes in $T_{1\rho}$ reverses between 30 °C and 25 °C (Table 2), indicating an effect of molecular motion on magnetization transfer under spin-locked conditions, we speculate that the viscosity of the glycerol solvent modulates either the ^{13}C chemical shifts or the conformation-dependent $^{3}J_{CC}$ coupling constants such as to increase the rate of transfer between particular pairs of nuclei. In AMP, the C1′–C4′ chemical shift difference is smaller, and the C2′–C3′ chemical shift difference is larger, than is typical in structured RNA oligonucleotides. Therefore, the $R_{1\rho}$ results in Table 2 and Figure 7 should not be taken as predictions of the specific effects that would be observed in RNA systems, but as indications that undesired transfers may occur under favorable combinations of conditions.

Discussion

Labeling schemes

The DL323 strain was designed to prevent metabolic scrambling of ^{13}C labels in metabolites derived from TCA cycle intermediates (LeMaster and Kushlan, 1996). For ribonucleotides, this strain should result in a clean alternate-site labeling pattern for the C5 and C6 atoms of pyrimidine rings, with the distribution of ^{13}C within the sugar ring dependent on the partitioning of carbon flux between the two possible routes to ribose-5-phosphate (see above). When grown on 2-^{13}C-glycerol, this strain yields a mixture of the 1′,4′-$^{13}C_2$ and 2′,4′-$^{13}C_2$ isotopomers of ribose, plus small amounts of minor species (Table 1). The ^{13}C4′–H4′ group is thus a fully isolated two-spin system, and at most 15% of the ^{13}C2′–H2′ groups have an interfering ^{13}C neighbor. Analysis of CMP multiplet patterns is consistent with specific labeling of the pyrimidine ring. This labeling pattern, which we refer to as (1′/2′,4′), thus yields a useful sample for analysis of multiple carbon sites with minimal interference from ^{13}C–^{13}C interactions. In many cases, however, more complete labeling at

individual sites will be desired, and we therefore explored the use of *zwf* strains of *E. coli* to restrict metabolism to a single route for the synthesis of ribose.

Our results indicate that *zwf* strains of *E. coli* grown on glycerol synthesize essentially all of their ribose-5-phosphate, and consequently their nucleotides, from three- and six-carbon precursors via the transketolase/transaldolase branch of the pentose phosphate pathway. When 2-^{13}C-glycerol is used as a carbon source, therefore, spectroscopically useful isolation of the C2′–H2′ and C4′–H4′ groups as two-spin systems is obtained, with the desired carbons labeled at 85% and >95%, respectively (Table 1). We note that, in this preparation, the ratio of 2′,4′-$^{13}C_2$-ribose to 4′-^{13}C-ribose is considerably higher than the 2:1 value expected based on the operation of this pathway in isolation (Figure 1b). We ascribe this effect to the depletion of the intermediate erythrose-1-phosphate for use in anabolic reactions including amino acid synthesis. The source of the small amount of residual label at C1′ is not clear at this time. This labeling pattern, which we term (2′,4′), is superior to the (1′/2′,4′) pattern obtained from DL323 *E. coli* in that a substantially higher fraction of C2′ sites contain label, increasing the signal-to-noise, and the minor 1′,2′,4′-$^{13}C_3$-ribose species is a smaller contributor to the total ^{13}C2′ population. Since (2′,4′)-NMPs allow relaxation studies of only two sites compared to the three with the (1′/2′,4′) pattern, however, we believe that both of these labeling schemes will have use in RNA spin relaxation studies. In any case, the (2′,4′) labeling scheme allows analysis of the C2′ and C4′ sites at full or nearly full occupancy and largely free of ^{13}C–^{13}C interference effects, thereby yielding essentially the ideal case for spin relaxation studies of these two carbons. This labeling pattern could be further refined by the supplementation of the medium with ^{13}C-formate, which has been shown to lead to high-level incorporation of ^{13}C at the C8 position of purines (Latham et al., 2005), potentially eliminating the need to prepare a separate uniformly labeled sample for analysis of purine ring dynamics.

Figure 4 illustrates another positive aspect of alternate-site labeling, in that the collapse of ribose peak triplets (for C2′, C3′, and C4′ peaks) into singlets has the potential to significantly alleviate spectral overlap in multidimensional NMR spectra. This effect is of particular importance in the crowded ribose region of the ^{1}H–^{13}C correlation spectrum. In uniformly labeled samples, multiplet collapse is typically obtained via the use of constant-time spectroscopy (Yamazaki et al., 1994), but at the cost of a substantial reduction in experimental sensitivity. The removal of multiplet contributions at the time of sample preparation alleviates the need for this expedient. The combination of alternate-site patterns with type-specific and/or segmental isotope labeling is expected to allow the application of spin relaxation studies to large RNA molecules. In preliminary work, we have resolved relaxation rates from essentially all cytosine C2′ and C4′ resonances in the 30-nucleotide lead-dependent ribozyme using Cyt-specific (2′,4′) labeling (J.E.J. and C.G.H., unpublished data).

Finally, we note that the incomplete labeling of C2′ on *zwf* bacteria grown on 2-^{13}C-glycerol implies that growth of this strain on 1,3-$^{13}C_2$-glycerol could give rise under some conditions to a significant level of 1′,2′,3′,5′-$^{13}C_4$-NMPs, potentially limiting the usefulness of such samples. One method for isolating the C3′–H3′ spin system is to derive ribonucleotides from wildtype *E. coli* grown on single-site labeled glucose. Glucose labeled with ^{13}C at each individual carbon atom is commercially available, albeit at considerable expense [4-^{13}C (99 %) glucose, for example, currently lists at $1600 for 1 g from Cambridge Isotope Laboratories, compared to $410/g for 2-^{13}C-glycerol and $638/g for 1,3-$^{13}C_2$-glycerol]. Due to the action of 6-phosphogluconate dehydrogenase, we expect ribonucleotides from this bacterial source to be labeled at the $(n-1)$ carbon of ribose (e.g., 3-^{13}C-ribose from 4-^{13}C glucose) (Parkin and Schramm, 1987; LoBrutto et al., 2001). We have grown wildtype *E. coli* (15224) on 4-^{13}C glucose and confirmed essentially complete labeling of the C3′ site with no detectable label elsewhere (Figure 5). This route thus provides a robust and selective, albeit costly, method to label a desired individual ribose carbon.

Removal of errors in measured relaxation rates

In the standard model-free scheme for the interpretation of relaxation rates in biomolecules, heteronuclear T_1, T_2 or $T_{1\rho}$, and NOE values are interpreted as arising from ^{1}H–X (X = ^{13}C or ^{15}N) dipole–dipole and X chemical-shift

anisotropy (CSA) relaxation mechanisms, along with possible contributions of μs-ms timescale conformational exchange to T_2 or $T_{1\rho}$. For an isolated ^{1}H–X two-spin system, this treatment is an excellent approximation as long as dipole–dipole/CSA cross-correlation effects are suppressed by the pulse sequence (Kay et al., 1989; Yamazaki et al., 1994). In the case of ^{13}C, however, the presence of strong scalar and dipolar couplings between the resonance of interest and directly bonded ^{13}C atoms gives rise to additional terms in the relaxation equations that substantially complicate the collection and/or interpretation of results (Yamazaki et al., 1994). For example, measured heteronuclear NOE values may be perturbed by the buildup of ^{1}H–^{13}C NOE on neighboring carbons followed by magnetization transfer via ^{13}C–^{13}C cross relaxation (Yamazaki et al., 1994). In this work, we have examined the effects of neighboring ^{13}C atoms on measured T_1 and $T_{1\rho}$ values in ribonucleotides.

In the case of longitudinal relaxation rates R_1 ($=1/T_1$) in the presence of directly bonded carbons, the autorelaxation rates ρ will contain, in addition to the ^{1}H–^{13}C dipolar and ^{13}C CSA contributions, dipole–dipole relaxation terms arising from ^{13}C–^{13}C interactions (ρ^{dd}_{c-c}) and, potentially, cross-correlation effects among the various dipole–dipole terms. In addition, ^{13}C–^{13}C cross-relaxation (σ_{c-c}) will affect the time course of relaxation during a T_1 experiment and may therefore either give rise to visibly multiexponential relaxation or, in subtler cases, affect the measured parameters. Both (ρ^{dd}_{c-c}) and σ_{c-c} rate constants contain spectral density terms J(0) evaluated at zero frequency and therefore will increase in magnitude relative to other contributions as the rotational correlation time τ_c of the molecule increases. Indeed, Bax and coworkers (Boisbouvier et al., 2003) showed analytically and experimentally that ^{13}C T_1 rates could be measured accurately in a uniformly labeled sample of a 12-base pair DNA dodecamer with correlation time 4 ns, but predicted the onset of unacceptable errors for molecules of correlation time 10 ns or above. The data presented in Table 2 and Figure 6 above bear this expectation out, as differences between R_1 values measured in specifically vs. uniformly labeled AMP of up to 25% at 12 ns τ_c and 100% at 17 ns τ_c are observed. (Interestingly, for the largest deviations, the observed rates in uniformly labeled AMP are actually lower than those in selectively labeled material, implying that the effects of cross-correlation and/or cross-relaxation dominate the increases in ρ arising from ρ^{dd}_{c-c} terms.) In other words, ribose ^{13}C T_1 values for typical RNA molecules of larger than roughly 40 nucleotides are untrustworthy if obtained on uniformly labeled samples. As NMR studies of RNA structure and dynamics are extended to molecules well above this threshold (Kim et al., 2002; Lukavsky et al., 2003; D'Souza et al., 2004), the necessity to overcome errors in T_1 measurements due to ^{13}C–^{13}C dipolar couplings will increase.

For the measurement of transverse relaxation rates, two distinct measurement schemes are possible. T_2 measurements based on the Carr-Purcell-Meiboom-Gill (CPMG) pulse scheme are completely unsuitable in the presence of ^{13}C–^{13}C couplings due to oscillatory behavior arising from echo modulation (Yamazaki et al., 1994). We have therefore applied the measurement of transverse relaxation under spin-locked conditions, or $T_{1\rho}$. For $T_{1\rho}$ measurements, the ^{1}H–^{13}C dipolar interaction itself depends on J(0) terms, and a strongly correlation-time dependent increase in the importance of ^{13}C–^{13}C dipolar contributions, as observed for T_1, is not expected. Instead, the greatest potential source of error is homonuclear Hartmann–Hahn (cross-polarization) transfer within the ^{13}C spin system during the spin-lock period (Yamazaki et al., 1994). In uniformly labeled DNA, this problem is moderated by the wide separation of chemical shifts for carbons at different sites; in the dodecamer studied by the Bax group, the closest approach is 8 ppm, between C4′ and C3′ (Boisbouvier et al., 2003), and accurate $T_{1\rho}$ measurements could be obtained. In RNA, by contrast, the possibilities for Hartmann–Hahn transfer are substantially greater. In the lead-dependent ribozyme, the median separation between C2′ and C3′ shifts is 2.6 ppm, and the ranges of the two carbon types actually overlap (Legault et al., 1998). The potential for chemical shift matching of two or more ^{13}C resonances within a ribose ring thus cannot be neglected, as shown in our $T_{1\rho}$ measurements (Table 2; Figure 7). These effects could be particularly troublesome in the use of relaxation dispersion studies to study μs-ms timescale exchange, as the Hartmann–Hahn effect will vary with spin-lock strength and therefore

could possibly yield an artifactual dependence of $T_{1\rho}$ on γB_1 that would be (wrongly) interpreted as indicating the presence of exchanging conformations. To analyze unambiguously, for example, slow interconversion of C3′-endo and C2′-endo conformations at the active sites of ribozymes, the use of alternate-site labeling or related schemes is thus an absolute necessity.[1] Finally, we note that CPMG-type T_2 measurements are preferable to $T_{1\rho}$ dispersion for detecting chemical exchange in some motional regimes (Akke, 2002). For these experiments, the use of uniformly labeled material is completely precluded, whereas the alternate-site labeled nucleotides should allow analysis in a straightforward fashion given the very small $^2J_{CC}$ values in these systems (Kline and Serianni, 1990; Hatala et al., 2001).

Perspective

The major alternative possibility to the alternate-site scheme for ribose carbon dynamics in RNA is the introduction of a low (10–20%) percentage of ^{13}C uniformly throughout the growth medium, termed random fractional labeling (Hines et al., 1993; Hines et al., 1994; Kojima et al., 1998; Boisbouvier et al., 1999). It is important to note that our labeling schemes are more efficient at removing ^{13}C–^{13}C interactions than even relatively stringent random-fractional patterns. For example, in a 15% fractionally labeled sample, 28% of ^{13}C–C2′ resonances have at least one directly bonded ^{13}C (C1′ or C3′), and 85% of the carbon of interest is NMR-silent. The effects of the undesired isotopomers may be removed via appropriate filters within the pulse sequence, but at a substantial further cost in sensitivity (Boisbouvier et al., 1999). Our (2′,4′) pattern, by contrast, yields essentially no residual ^{13}C–^{13}C interactions, with a 5-fold or more advantage in sensitivity due to the higher percentage of labeling. The (1′/2′,4′) pattern, allowing analysis of three sites in a single sample, has 10% or less residual ^{13}C–^{13}C interaction and a two-fold advantage in sensitivity at C2′, along with a six-fold advantage in sensitivity and essentially perfect isolation at C4′. We believe that alternate-site labeling will be preferred to random-fractional labeling for most if not all applications.

Vallurupalli and Kay (2005) recently introduced an elegant suite of experiments to analyze ribose dynamics using ^2H relaxation rates measured in 100%-^{15}N,^{13}C/50%-^2H RNA samples. These experiments form a valuable complement to ^{13}C relaxation rates measured with the scheme introduced here, since ^2H and ^{13}C relaxation probe distinct internal-motion spectral density functions. In addition, ^2H relaxation is relatively insensitive to chemical exchange contributions. This can be advantageous in "model-free" analyses of sub-ns motion, but also means that ^{13}C labeling approaches are more suitable for relaxation dispersion studies of exchange processes on longer time scales.

In short, we have used a convenient biosynthetic procedure to prepare ribonucleotides with favorable ^{13}C labeling patterns for NMR spin relaxation studies of the ribose rings in nucleic acids. Using relaxation measurements for monomer samples at varying correlation times, we have demonstrated that magnetic interactions with adjacent ^{13}C nuclei are indeed a substantial source of error in T_1 measurements for larger nucleic acid molecules and in $T_{1\rho}$ measurements in RNA systems. The alternate-site labeling pattern is a practical approach to removing these errors. By allowing the NMR study of spin relaxation in RNA to be generalized from the currently studied nucleotide base moieties to the ribose backbone, the methods reported in this paper will open a new window into RNA conformational dynamics and advance our efforts to understand the coupling between dynamics and function in ribozymes and other systems.

Acknowledgements

The authors are grateful to David LeMaster for helpful discussions, to John SantaLucia for comments on the manuscript, and to the Coli Genetic Stock Center (Yale) for bacterial strains. This

[1] In 2′,4′-$^{13}C_2$ nucleotides, the two-bond scalar coupling between C2′ and C4′, $^2J_{CC}$, is still present and in principle could affect the measurements. However, this coupling has been measured at 0.8 Hz using chemically synthesized 2-deoxyribonolactone derivatives (Hatala et al., 2001) and at 0.9 Hz in adenosine (Kline and Serianni, 1990), and therefore may be taken as negligible for the purposes of the present experiments. For 1′,4′-$^{13}C_2$ nucleotides, the value of the three-bond coupling between C1′ and C4′ will be conformation-dependent, but the relatively large chemical shift difference between these two carbon types in oligonucleotides makes significant Hartmann–Hahn transfer unlikely.

work was supported by faculty startup funds and an Intramural Research Program Grant from Michigan State University and by the National Institutes of Health (GM-069742).

References

Akke M. (2002) *Curr. Opin. Struct. Biol.*, **12**, 642–647.

Akke M., Fiala R., Jiang F., Patel D. and Palmer A.G. III (1997) *RNA*, **3**, 702–709.

al-Hashimi H.M. (2005) *Chembiochem*, **6**, 1506–1519.

Batey R.T., Battiste J.L. and Williamson J.R. (1995) *Methods Enzymol.*, **261**, 300–322.

Batey R.T., Inada M., Kujawinski E., Puglisi J.D. and Williamson J.R. (1992) *Nucl. Acids. Res.*, **20**, 4515–4523.

Bax A. and Davis D.G. (1985) *J. Magn. Reson.*, **63**, 207–213.

Blad H., Reiter N.J., Abildgaard F., Markley J.L. and Butcher S.E. (2005) *J. Mol. Biol.*, **353**, 540–555.

Boisbouvier J., Brutscher B., Simorre J.-P. and Marion D. (1999) *J. Biomolec. NMR*, **14**, 241–252.

Boisbouvier J., Wu Z., Ono A., Kainosho M. and Bax A. (2003) *J. Biomolec. NMR*, **27**, 133–142.

Borer P.N., LaPlante S.R., Anil Kumar, Zanatta N., Martin A., Hakkinen A. and Levy G.C. (1994) *Biochemistry*, **33**, 2441–2450.

Bryce D.L., Grishaev A. and Bax A. (2005) *J. Am. Chem. Soc.*, **127**, 7387–7396.

Castellani F., van Rossum B., Diehl A., Schubert M., Rehbein K. and Oschkinat H. (2002) *Nature*, **420**, 98–102.

Castellani F., van Rossum B.J., Diehl A., Rehbein K. and Oschkinat H. (2003) *Biochemistry*, **42**, 11476–11483.

Catoire L.J. (2004) *J. Biomol. NMR*, **28**, 179–184.

D'Souza V., Dey A., Habib D. and Summers M.F. (2004) *J. Mol. Biol.*, **337**, 427–442.

Dayie K.T., Brodsky A.S. and Williamson J.R. (2002) *J. Mol. Biol.*, **317**, 263–278.

Dayie K.T., Wagner G. and Lefèvre J.F. (1996) *Annu. Rev. Phys. Chem.*, **47**, 243–282.

Duchardt E. and Schwalbe H. (2005) *J. Biomol. NMR*, **32**, 295–308.

Ebrahimi M., Rossi P., Rogers C. and Harbison G.S. (2001) *J. Magn. Reson.*, **150**, 1–9.

Edwards J.S. and Palsson B.O. (2000) *Proc. Natl. Acad. Sci. USA*, **97**, 5528–5533.

Fraenkel D.G. (1968) *J. Bacteriol.*, **95**, 1267–1271.

Gaudin F., Chanteloup L., Thuong N.T. and Lancelot G. (1997) *Magn. Reson. Chem.*, **35**, 561–565.

Gaudin F., Paquet F., Chanteloup L., Beau J.-M., Thuong N.T. and Lancelot G. (1995) *J. Biomolec. NMR*, **5**, 49–58.

Hall K.B. and Tang C. (1998) *Biochemistry*, **37**, 9323–9332.

Hatala P.J., Kallmerten J. and Borer P.N. (2001) *Nucleosides Nucleotides Nucleic Acids*, **20**, 1961–1973.

Hines J.V., Landry S.M., Varani G. and Tinoco I. (1994) *J. Am. Chem. Soc.*, **116**, 5823–5831.

Hines J.V., Varani G., Landry S.M. and Tinoco I. (1993) *J. Am. Chem. Soc.*, **115**, 11002–11003.

Hoffman D.W. and Holland J.A. (1995) *Nucl. Acids. Res.*, **23**, 3361–3362.

Hoogstraten C.G., Legault P. and Pardi A. (1998) *J. Mol. Biol.*, **284**, 337–350.

Hoogstraten C.G., Wank J.R. and Pardi A. (2000) *Biochemistry*, **39**, 9951–9958.

Isaacs R.J., Rayens W.S. and Spielmann H.P. (2002) *J. Mol. Biol.*, **319**, 191–207.

Isaacs R.J. and Spielmann H.P. (2001) *J. Mol. Biol.*, **307**, 525–540.

Kay L.E., Torchia D.A. and Bax A. (1989) *Biochemistry*, **28**, 8972–8979.

Ke A., Zhou K., Ding F., Cate J.H. and Doudna J.A. (2004) *Nature*, **429**, 201–205.

Kim I., Lukavsky P.J. and Puglisi J.D. (2002) *J. Am. Chem. Soc.*, **124**, 9338–9339.

King G.C., Harper J.W. and Xi Z. (1995) *Methods. Enzymol.*, **261**, 436–450.

Kishore A.I., Mayer M.R. and Prestegard J.H. (2005) *Nucleic Acids Res.*, **33**, e164 .

Kline P.C. and Serianni A.S. (1990) *J. Am. Chem. Soc.*, **112**, 7373–7381.

Klooster W.T., Ruble J.R. and Craven B.M. (1991) *Acta. Crystallogr., B.*, **47**, 376–383.

Kojima C., Ono A., Kainosho M. and James T.L. (1998) *J. Magn. Reson.*, **135**, 310–333.

Kojima C., Ulyanov N.B., Kainosho M. and James T.L. (2001) *Biochemistry*, **40**, 7239–7246.

Latham M.P., Brown D.J., McCallum S.A. and Pardi A. (2005) *Chembiochem*, **6**, 1492–1505.

Legault P., Hoogstraten C.G., Metlitzky E. and Pardi A. (1998) *J. Mol. Biol.*, **284**, 325–335.

LeMaster D.M. and Cronan J.E. Jr. (1982) *J. Biol. Chem.*, **257**, 1224–1230.

LeMaster D.M. and Kushlan D.M. (1996) *J. Am. Chem. Soc.*, **118**, 9255–9264.

LoBrutto R., Bandarian V., Magnusson O.T., Chen X.Y., Schramm V.L. and Reed G.H. (2001) *Biochemistry*, **40**, 9–14.

Lukavsky P.J., Kim I., Otto G.A. and Puglisi J.D. (2003) *Nat. Struct. Biol.*, **10**, 1033–1038.

Nelson D.L. and Cox M.M. (2004) *Lehninger Principles of Biochemistry*, W.H. Freeman, New York.

Nikonowicz E.P., Sirr A., Legault P., Jucker F.M., Baer L.M. and Pardi A. (1992) *Nucleic Acids Res.*, **20**, 4507–4513.

Palmer A.G., Kroenke C.D. and Loria J.P. (2001) *Methods Enzymol.*, **339**, 204–238.

Palmer A.G. III (2004) *Chem. Rev.*, **104**, 3623–3640.

Parkin D.W. and Schramm V.L. (1987) *Biochemistry*, **26**, 913–920.

Perez-Canadillas J.M. and Varani G. (2001) *Curr. Opin. Struct. Biol.*, **11**, 53–58.

Pley H.W., Flaherty K.M. and McKay D.B. (1994) *Nature*, **372**, 68–74.

Rossi P. and Harbison G.S. (2001) *J. Magn. Reson.*, **151**, 1–8.

SantaLucia J., Shen L.X., Cai Z.P., Lewis H. and Tinoco I. (1995) *Nucleic Acids Res.*, **23**, 4913–4921.

Shajani Z. and Varani G. (2005) *J. Mol. Biol.*, **349**, 699–715.

Spielmann H.P. (1998) *Biochemistry*, **37**, 16863–16876.

Szyperski T., Luginbühl P., Otting G., Güntert P. and Wüthrich K. (1993) *J. Biomolec. NMR*, **3**, 151–164.

Treiber D.K. and Williamson J.R. (2001) *Curr. Opin. Struct. Biol.*, **11**, 309–314.

Vallurupalli P. and Kay L.E. (2005) *J. Am. Chem. Soc.*, **127**, 6893–6901.

Wagner G. and Wüthrich K. (1986) *Methods Enzymol.*, **131**, 307–326.

Williamson J.R. and Boxer S.G. (1989) *Biochemistry*, **28**, 2819–2831.

Yamazaki T., Muhandiram D.R. and Kay L.E. (1994) *J. Am. Chem. Soc.*, **116**, 8266–8278.